

# Topography of ion-etched Corning 7059 glass

MARIAN LUKASZEWICZ, ZBIGNIEW W. KOWALSKI  
*Technical University of Wroclaw, 50-370 Wroclaw, Poland*

Topographs of Corning 7059 glass, developed by 7 kV, 70  $\mu\text{A}$   $\text{Ar}^+$  irradiation from a hollow anode ion gun were investigated. Two forms of surface topography were observed: lens-shaped cavities and waves. These are discussed in terms of measured sputtering yield against incidence angle relation or beam divergence. Practical applications in specimen preparation for transmission electron microscopy and glass homogeneity testing are suggested.

## 1. Introduction

Glass is commonly used as a substrate material for thin film circuits. Miniaturization in electronics needs new processes and investigation methods with a high dimensional resolution. Ion sputtering of thin films has already found an application in modern lithography while ion thinning of the substrate enables direct transmission electron microscopy (TEM) observation of deposit. In both cases the knowledge of sputtering parameters of the substrate material is very useful. Due to the complicated compositions and varieties of glasses, theoretical considerations are not very helpful in practice. The published experimental results shown in Table I are far from complete [1-10]. Under such circumstances it seems that reasonable experimental testing on ion etching, with a fixed sample and perpendicular incidence, could assist in understanding the same sample preparation using the same ion source in more sophisticated conditions.

## 2. Experimental conditions

### 2.1. Ion source

A simple glow discharge ion source [11-13] was used in our experiments. This hollow anode gun, with its anode and cathode holes having 4 and 1 mm diameters, respectively, and an anode-cathode spacing of 1.5 mm, functioned in an argon atmosphere at 7 kV. A beam current collected (Faraday cage) at the cathode potential recorded a total current of about 70  $\mu\text{A}$ . At a distance of 10 mm from the cathode this resulted in a maximum current density of about 500  $\mu\text{A cm}^{-2}$ .

The extracted beam enabled the etching of conducting materials to take place. Tantalum was used for the cathode because of its high sputtering resistance quality. Fig. 1 shows a diagram of the ion bombardment system.

### 2.2. Target

Corning 7059 glass in the form of a plate 2 cm  $\times$  3 cm  $\times$  0.09 cm was examined. Due to the small alkaline ion content, this substrate material assures a high resistance stability of deposit. Its surface is smooth (a peak-to-valley distance of less than 250  $\text{\AA}$ ) and it has a high softening point (827 $^{\circ}$ C). Taking into account the beam parameters (a maximum energy flux of about 3  $\text{W cm}^{-2}$ , total power about 0.5 W) and heat conduction through the glass plate, a maximum temperature of just under 150 $^{\circ}$ C can be estimated. Under similar conditions Dhariwal and Fitch [9] measured an increase in temperature up to 135 $^{\circ}$ C. An examination of the etched plate with polarized light has not shown any stresses which would normally be present in cases of exposure to high temperatures and considerable temperature gradients.

### 2.3. Surface topography investigation methods

A profile of the funnel formed on the plate due to ion erosion was recorded on a profilograph. The maximum depth,  $d$ , of the funnel was measured at various angles,  $\theta$ , of ion beam incidence for a fixed ion bombardment time. From the resulting expression,  $d \sim S(\theta) \cos \theta$ , the values of  $S(\theta) \cos \theta$

TABLE I Ion etching of glass – conditions and results

Ion source	Beam characteristic	Target material	Incident angle	Rotation	Observed topographic forms	References
Hollow anode	air, 4 kV	Sodium-calcium Glass	$\theta = 0^\circ$ $20^\circ < \theta < 60^\circ$	No No	Hummocks Parallel grooves perpendicular to the beam (waves)	[1]
*	Ar <sup>+</sup> , 50 kV 10 mA cm <sup>-2</sup>	Fused silica	$\theta > 75^\circ$ $\theta = 0^\circ$ $\theta = 85^\circ$	No No No	Parallel grooves along the beam Pitted surface Striated surface	[2]
Hollow anode	*	Silica glass	*	*	Hummocks	[3]
Hollow anode	Ar <sup>+</sup> , 6 kV 20 $\mu$ A cm <sup>-2</sup>	Fused silica Glass	$\theta \geq 0^\circ$ $\theta \sim 0^\circ$	Yes No	Hummocks Absence of hummocks	[4, 5]
*	N <sup>+</sup> , 20 kV 10 $\mu$ A cm <sup>-2</sup>	Corning 7059	$\theta = 50^\circ$	No	Cones	[6]
*	Ar <sup>+</sup> , 20 kV 30 $\mu$ A cm <sup>-2</sup>	Silica glass	$\theta = 0^\circ$	No	Depressions, steps, terraces	[7]
*	Xe <sup>+</sup>	Glass	$\theta = 45^\circ$	No	Periodic structure	[8]
Saddle field	Ar <sup>+</sup> , 6–8 kV 500 $\mu$ A cm <sup>-2</sup>	Soda-glass	$\theta = 27^\circ$	No	Parallel grooves along the beam	[9]
Nielsen	Ar <sup>+</sup> , Ne <sup>+</sup> 50 kV	Glass	$\theta = 0^\circ$	*	Blisters, surface crystallization	[10]

\*No data.

$S(0)$  were calculated. Microrelief details were observed by TEM (binary carbon replicas method) or by scanning electron microscopy (SEM). The distributions of microrelief forms and possible stresses were examined using an optical microscope.

### 3. Results and discussion

After 1 h of ion etching under the conditions described above, a funnel-shaped pit could be observed on the glass surface. The profile of the funnel and true inclination of its slopes are depicted in Fig. 2. The axial symmetry of the funnel is

typical of perpendicular ion beam incidence. The funnel profile for  $\theta = 0$  corresponds to the measured ion current density distribution (movable wire probes, diameters 0.1 and 0.8 mm were used for measurements). Microscopic methods (see Section 2.3) have shown that in addition to a macroscopic effect (funnel), microscopic relief forms develop: lens cavities and waves. Lens cavities, shown in Figs 3, 4 and 5 show unexpected axial symmetry. The diameters of these cavities

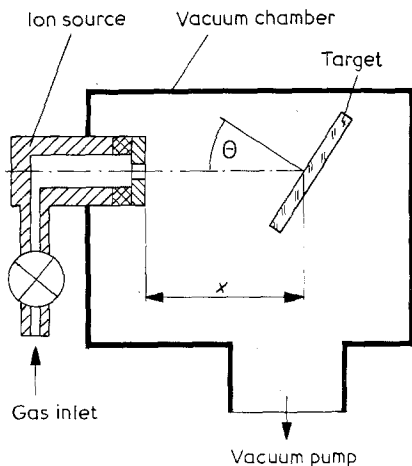


Figure 1 Scheme of ion bombardment system;  $x$  is the ion gun-sample distance,  $\theta$  is the incidence angle.

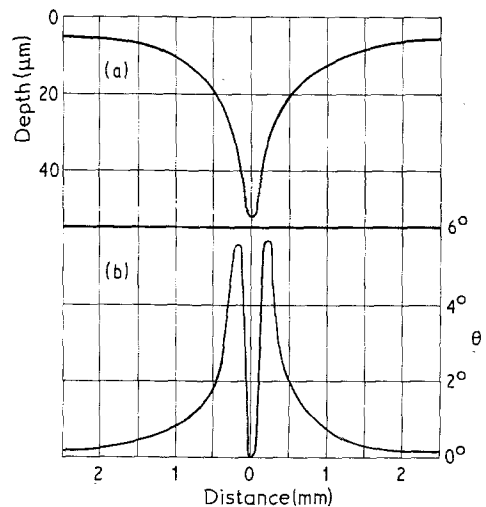


Figure 2 The funnel due to the perpendicular beam etching for 1 h at  $x = 10$  mm; (a) funnel profile, (b) true inclination of the slope.

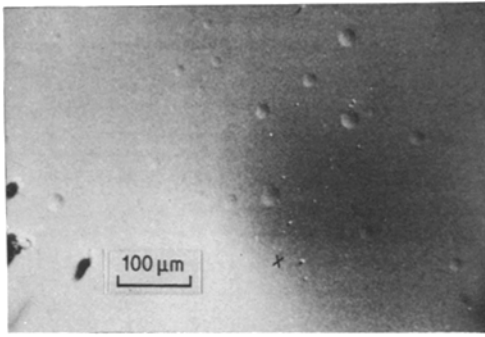


Figure 3 SEM image of the funnel centre region with lens-shaped cavities. The funnel has a similar type of shadow as the cavities. X is the funnel centre.

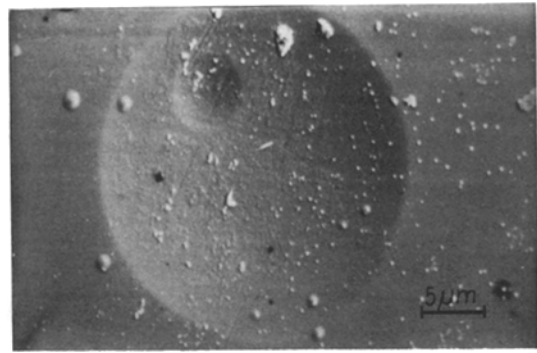


Figure 4 SEM of the superposition of the lens cavities in the neighbourhood of the funnel centre.

reach up to  $25\ \mu\text{m}$  in the neighbourhood of the funnel centre and decrease as the distance from the funnel centre increases. They take up as much as 2% of the total etched surface. The small diameter cavities have sharply outlined shadows observed in TEM by the replica method (Fig. 5a). The contrast of the cavities without shadows decreases with an increase in diameter (compare Fig. 5a and b). This means that lens cavities grow faster in horizontal directions than in vertical directions. As a consequence of the  $S(\theta) \cos \theta/S(0)$  function [14, 15] their initial depth is preserved as material at the bottom of the cavity has the same erosion rate as the rest of the  $0^\circ$  oriented surface. Fig. 6 shows this function resultant from Bach's [16] and our findings (compare Section 2.3). The ratio of horizontal speed,  $v_h$ , of the moving cavity edge to the etch speed,  $v_v$ , of the surface normal to the beam (Fig. 7) was calculated for Corning 7059 glass. In accordance with this function the small cavities with an angle  $\theta \approx 60^\circ$  will grow most rapidly in a horizontal direction.

The problem of primary cavity origin is still an open one. It seems that they are due to local heterogeneities in bulk glass (e.g. microbubbles). If their initial forms have an angle of  $\theta \approx 90^\circ$ , then the secondary processes of redeposition or ion scattering must also be responsible for growing and shaping. Superposition of cavities (Figs 4 and 5a) as well as the fact that bigger and more numerous cavities arise in more intensively etched regions provides a proof for the above interpretation.

In the ring region surrounding the funnel different forms such as waves were observed (Figs 8 and 9). They lay approximately perpendicular to the radius from the funnel centre. The waves become visible 2.5 mm from the funnel centre and gradually disappear 3.0 mm from the funnel centre. The wave period is approximately 75 nm. The wave regularity is interrupted by many disturbances. It is possible to observe local disappearance of waves (Fig. 8a), interruptions in strange forms (Fig. 8b) and single islands with an undulating surface (Fig. 9). In the wave region lens cavities are not observed. Waves with a similar

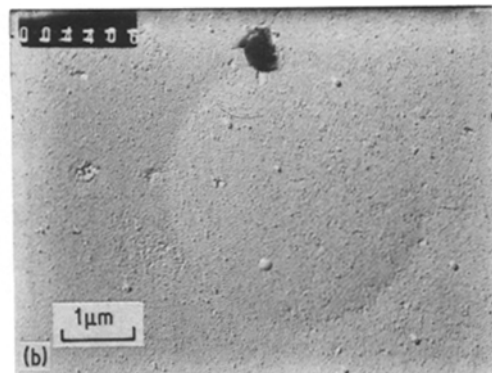
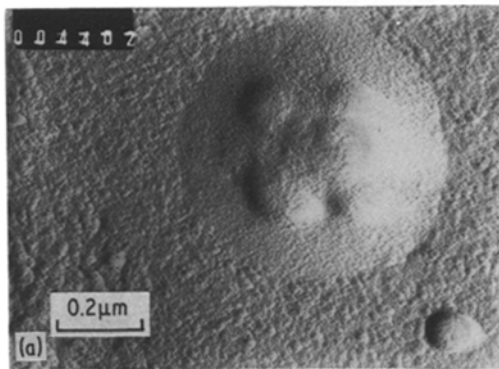


Figure 5 TEM replica of the lens cavities in the neighbourhood of the funnel centre, (a) relatively deep small cavities, (b) big flat cavity.

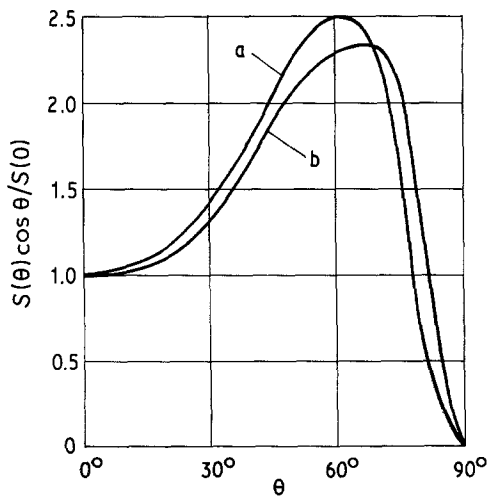


Figure 6  $S(\theta) \cos \theta / S(0)$  function against angle of incidence  $\theta$  for  $\text{Ar}^+$  ions on: (a) Corning 7059 glass (our results), (b) silica glass [15].

period and shape were obtained by Navez *et al.* [1] at an ion incidence angle of  $\theta = 30^\circ$  to the normal. This result concurrence suggests that in this case the process is weakly dependent on material and ion parameters (they supplied their ion gun with air and used soda-lime glass for the target). The origin of wave formation lies in oblique incidence. In our case, in the wave region, the ion incidence angle due to the geometrical beam divergence is less than  $15^\circ$ . However it is possible that as a result of repulsion by the electrical charge in the central region of the bombarded area the real incidence angle will be enlarged.

#### 4. Conclusions

The ion gun used in our experiments enabled a quick etching of glass or alumina ceramics (some

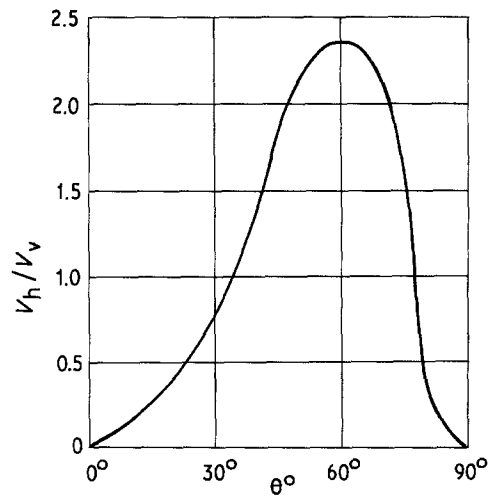


Figure 7 Angular dependence of  $v_h/v_v$  function;  $v_h$  is the horizontal speed and  $v_v$  is the vertical speed.

tens of micrometres per hour at a distance of 10 mm). The shape of the central funnel is a reflection of the beam density distribution. The observed microscopic effects such as lens cavities and waves are not fully explained in the literature (lens cavities are not among the typical forms of ion etched glass surfaces presented in Table I). Though harmful in the case of specimen preparation for TEM, lens cavities may be useful in the estimation of heterogeneity density in glass, assuming that they occur for that reason alone. This must be proved by *in situ* ion etching microscopic observation. The waves were not harmful to TEM preparations in our case because they lay in the border region of a typical TEM sample (3 mm in diameter). They give qualitative information about ion beam symmetry, divergence and stability.

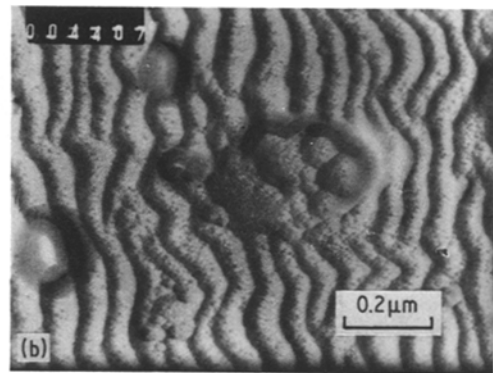
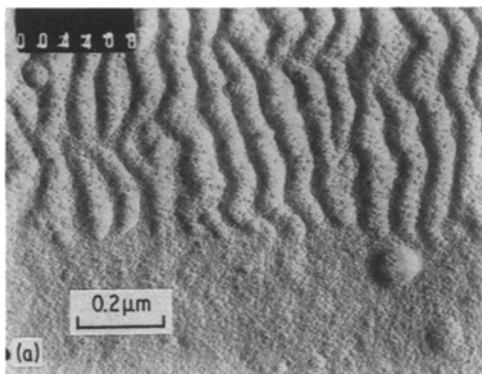


Figure 8 TEM of waves 2.5 to 3 mm out from the funnel centre, (a) local disappearance of waves, (b) interruptions by heterogeneities.

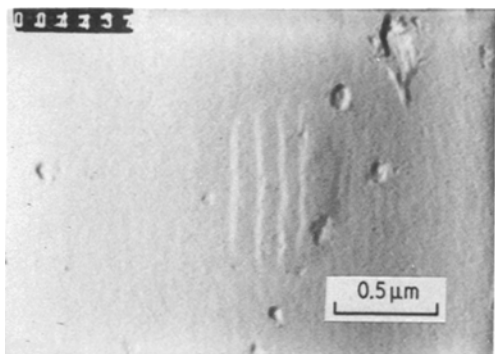


Figure 9 TEM of a "wave packet" in the same region as shown in Fig. 8.

### Acknowledgement

We would like to thank Doctor J. Zdanowski (Technical University of Wrocław) for his suggestions in the preparation of this paper.

### References

1. M. NAVEZ, C. SELLA and D. CHAPEROT, Colloques Internationaux CNRS, Bellevue, December, 1962, p. 233.
2. M. TARASEVICH, *Appl. Opt.* **9** (1970) 173.
3. D. J. BARBER, *Beitr. elektronenmikroskop. Direktabb. Oberfl.* **5** (1972) 585.
4. D. J. BARBER, Proceedings of the Fifth European Congress on Electron Microscopy, 1972, 302.
5. I. S. T. TSONG and D. J. BARBER, *J. Mater. Sci.* **7** (1972) 687.
6. A. R. BAYLY and P. D. TOWNSEND, *J. Phys. D: Appl. Phys.* **5** (1972) L103.
7. A. R. BAYLY, *J. Mater. Sci.* **7** (1972) 404.
8. R. S. NELSON and D. J. MAZEY, *Rad. Eff.* **18** (1973) 127.
9. R. S. DHARIWAL and R. K. FITCH, *J. Mater. Sci.* **12** (1977) 1225.
10. B. RAUSCHENBACH and W. HINZ, *Phys. Stat. Sol. (a)* **47** (1978) 79.
11. M. PAULUS and F. REVERCHON, *J. Phys. Radium, Phys. Appl. Suppl.* **22** (1961) 103A.
12. L. HOLLAND, R. E. HURLEY and L. LAURENSEN, *J. Phys. E, Sci. Instrum.* **4** (1971) 198.
13. C. G. CROCKETT, *Vacuum* **23** (1973) 11.
14. D. J. BARBER, F. C. FRANK, M. MOSS, J. W. STEEDS and I. S. T. TONG, *J. Mater. Sci.* **8** (1973) 1030.
15. G. CARTER, J. S. COLLIGON and M. J. NOBES, *ibid.* **8** (1973) 1473.
16. H. BACH, *J. Non-Cryst. Solids* **3** (1970) 1.

Received 6 March and accepted 30 June 1980.